Research Article | Vol. 25, No. 3 | 6 Feb 2017 | OPTICS EXPRESS 2752
Optics EXPRESS

Robust sub-millihertz-level offset locking for transferring optical frequency accuracy and for atomic two-photon spectroscopy

WANG-YAU CHENG,* TING-JU CHEN,CHIA-WEI LIN, BO-WEI CHEN, YA-PO YANG, AND HUNG YI HSU

Department of Physics, National Central University, Taoyuan, 32001, Taiwan
**wycheng@ncu.edu.tw*

Abstract: Robust sub-millihertz-level offset locking was achieved with a simple scheme, by which we were able to transfer the laser frequency stability and accuracy from either cesium-stabilized diode laser or comb laser to the other diode lasers who had serious frequency jitter previously. The offset lock developed in this paper played an important role in atomic two-photon spectroscopy with which record resolution and new determination on the hyperfine constants of cesium atom were achieved. A quantum-interference experiment was performed to show the improvement of light coherence as an extended design was implemented.

OCIS codes: (140.3425) Laser stabilization; (020.4180) Multiphoton processes.

References and links

1. L. Cacciapuoti, M. de Angelis, M. Fattori, G. Lamporesi, T. Petelski, M. Prevedelli, J. Stuhler, and G. M. Tino, "Analog+digital phase and frequency detector for phase locking of diode lasers," Rev. Sci. Instrum. **76**(5), 053111 (2005).
2. W. Peng, L. Zhou, S. Long, J. Wang, and M. Zhan, "Locking laser frequency of up to 40 GHz offset to a reference with a 10 GHz electro-optic modulator," Opt. Lett. **39**(10), 2998–3001 (2014).
3. D. Höckel, M. Scholz, and O. Benson, "A robust phase-locked diode laser system for EIT experiments in cesium," Appl. Phys. B **94**(3), 429–435 (2009).
4. A. M. Marino and C. R. Stroud, "Phase-locked laser system for use in atomic coherence experiments," Rev. Sci. Instrum. **79**(5), 013104 (2009).
5. S. M. Foreman, A. D. Ludlow, M. H. G. de Miranda, J. E. Stalnaker, S. A. Diddams, and J. Ye, "Coherent optical phase transfer over a 32-km fiber with 1 s instability at 10^{-17}," Phys. Rev. Lett. **99**(15), 153601 (2007).
6. N. Beverini, M. Prevedelli, F. Sorrentino, B. Nyushkov, and A. Ruffini, "An analog+digital phase-frequency detector for phase locking of a diode laser to an optical frequency comb," Quantum Electron. **34**(6), 559–564 (2004).
7. N. Scharnhorst, J. B. Wübbena, S. Hannig, K. Jakobsen, J. Kramer, I. D. Leroux, and P. O. Schmidt, "High-bandwidth transfer of phase stability through a fiber frequency comb," Opt. Express **23**(15), 19771–19776 (2015).
8. T. R. Schibli, I. Hartl, D. F. C. Yost, M. J. Martin, A. Marcinkevicius, M. E. Fermann, and J. Ye, "Optical frequency comb with submillihertz linewidth and more than 10 W average power," Nat. Photonics **2**(6), 355–359 (2008).
9. J. Ye and J. L. Hall, "Optical phase locking in the microradian domain: potential applications to NASA spaceborne optical measurements," Opt. Lett. **24**(24), 1838–1840 (1999).
10. F. Herzog, K. Kudielka, D. Erni, and W. Bächtold, "Optical phase locked loop for transparent inter-satellite communications," Opt. Express **13**(10), 3816–3821 (2005).
11. C. H. Henry, "Theory of the linewidth of semiconductor lasers," IEEE J. Quantum Electron. **18**(2), 259–264 (1982).
12. Z. Xu, X. Zhang, K. Huang, and X. Lu, "A digital optical phase-locked loop for diode lasers based on field programmable gate array," Rev. Sci. Instrum. **83**(9), 093104 (2012).
13. A. Schwettmann, J. Sedlacek, and J. P. Shaffer, "Field-programmable gate array based locking circuit for external cavity diode laser frequency stabilization," Rev. Sci. Instrum. **82**(10), 103103 (2011).
14. T. Day, E. Gustafson, and R. Byer, "Sub-Hertz relative frequency stabilization of two-diode laser-pumped Nd:YAG lasers locked to a Fabry-Perot Interferometer," IEEE J. Quantum Electron. **28**(4), 1106–1117 (1992).
15. Our power splitters were from Mini-circuit, model ZSCQ-2–90 and ZMSCQ-2–50 +
16. Tektronix Inc. model: RSA3408A real time spectrum analyzer.
17. M. Prevedelli, T. Freegarde, and T. W. Hansch, "Phase lock of grating-tuned diode lasers," Appl. Phys. B **60**, S241–S248 (1995).

#281418 https://doi.org/10.1364/OE.25.002752
Journal © 2017 Received 25 Nov 2016; revised 18 Jan 2017; accepted 22 Jan 2017; published 2 Feb 2017

Optics EXPRESS

18. Y. H. Chen, T. W. Liu, C. M. Wu, C. C. Lee, C. K. Lee, and W. Y. Cheng, "High-resolution 133Cs 6S-6D, 6S-8S two-photon spectroscopy using an intracavity scheme," Opt. Lett. **36**(1), 76–78 (2011).
19. M. Zhu and J. L. Hall, "Stabilization of optical phase/frequency of a laser system: application to a commercial dye laser with an external stabilizer," J. Opt. Soc. Am. B **10**(5), 802–816 (1993).
20. C.-M. Wu, T. W. Liu, M. H. Wu, R. K. Lee, and W. Y. Cheng, "Absolute frequency of cesium 6S-8S 822 nm two-photon transition by a high-resolution scheme," Opt. Lett. **38**(16), 3186–3189 (2013).
21. A. Kortyna, N. A. Masluk, and T. Bragdon, "Measurement of the $6d^2D_J$ hyperfine structure of cesium using resonant two-photon sub-Doppler spectroscopy," Phys. Rev. A **74**(2), 022503 (2006).
22. T. Ohtsuka, N. Nishimiya, T. Fukuda, and M. Suzuki, "Doppler-free two-photon spectroscopy of $6S_{1/2}$-$6D_{3/2,5/2}$ transition in cesium," J. Phys. Soc. Jpn. **74**(9), 2487–2491 (2005).
23. Symmetricom 5071a cesium clock whose frequency was traced to UTC(TL) via the flying clock method and that resulted in 1.4×10^{-14} one-day accuracy and 10^{-11} for 10 second sampling time; UTC: Coordinated Universal Time; TL: Telecommunication laboratories of Taiwan.
24. D. A. Steck, "Rubidium 87 D line Data," revision 1.6, 14 October 2003, http://steck.us/alkalidata/
25. D. Touahri, O. Acef, A. Clairon, J.-J. Zondy, R. Felder, L. Hilico, B. de Beauvoir, F. Birben, and F. Nez, "Frequency measurement of the $5S_{1/2}$(F=3)-$5D_{5/2}$ (F=5) two-photon transition in rubidium," Opt. Commun. **133**(96), 471–478 (1997).
26. M. Poulin, C. Latrasse, D. Touahri, and M. Tetu, "Frequency stability of an optical frequency standard at 192.6 THz based on a two-photon transition of rubidium atoms," Opt. Commun. **207**(2), 233–242 (2002).
27. C. S. Edwards, G. P. Barwood, H. S. Margolis, P. Gill, and W. R. C. Rowley, "Development and absolte frequency measurement of a pair of 778 nm two-photon rubidium standards," Metrologia **42**(5), 464–467 (2005).
28. T. J. Quinn, "Practical realization of the definition of the metre, including recommend radiations of other optical frequency standards," Metrologia **40**(2), 103–133 (2003).
    T. J. Quinn, "Mise en pratique of the definition of the Metre," Metrologia **36**, 211 (1999).
29. U. Schünemann, H. Engler, R. Grimm, M. Weidemuller, and M. Zielonkowski, "Simple scheme for tunable frequency offset locking of two lasers," Rev. Sci. Instrum. **70**(1), 242–243 (1999).
30. Filter from K&L model 3TNF-30/76-N/N.
31. J. H. Shirley, "Modulation transfer processes in optical heterodyne saturation spectroscopy," Opt. Lett. **7**(11), 537–539 (1982).
32. C. Affolderbach, A. Nagel, S. Knappe, C. Jung, D. Wiedenmann, and R. Wynands, "Nonlinear spectroscopy with a vertical-cavity surface-emitting laser (VCSEL)," Appl. Phys. B **70**(3), 407–413 (2000).
33. C. Y. Ye and A. S. Zibro, "Width of the electromagnetically induced transparency resonance in atomic vapor," Phys. Rev. A **65**(2), 023806 (2002).
34. Y. Li and M. Xiao, "Observation of quantum interference between dressed states in an electromagnetically induced transparency," Phys. Rev. A **51**(6), 4959–4962 (1995).
35. R. L. Barger and J. L. Hall, "Pressure shift and broadening of methane line at 3.39 μ studied by laser-saturated molecular absorption," Phys. Rev. Lett. **22**(1), 4–8 (1969).
36. C.-Y. Cheng, C.-M. Wu, G.-B. Liao, and W.-Y. Cheng, "Cesium $6S_{(1/2)} \rightarrow 8S_{(1/2)}$ two-photon-transition-stabilized 822.5 nm diode laser," Opt. Lett. **32**(5), 563–565 (2007).
37. J. Ye, L. S. Ma and J. L. Hall, "Molecular iodine clock," Phys. Rev. Lett. **87**(27), 270801 (2001).

1. Introduction

Optical offset locking plays a very important role in many AMO (Atomic, Molecular and Optical Physics) experiments. For example, it is useful in the red-detuning of a laser in cooling-atom experiments [1,2], bridging the frequency gap between two atomic transitions in electromagnetically induced transparency (EIT) experiments [3,4], transferring the frequency accuracy from a comb laser to various CW lasers in metrology applications [5–8], and optical phase comparison and communication in space science [9,10]. Among the aforementioned applications, some high-precision experiments particularly require sub-millihertz (mHz)-level offset locking, such as in quantum optics [4], optical clockwork [5–8], and space-based measurements [9], in which an analog phase-sensitive detector was a mainstay in their delicate experimental setups. This is because the analog phase detector has benefits of lower phase noise and faster error-signal response, compared to those of digital phase-frequency detectors in which the "edge-trigger" causes digitizing noise and the "flip-flop" causes time delay. Unfortunately, an analog phase detector such as a mixer cannot support a suitable capture range for laser locking when the laser beat frequency changes drastically (jitter), a situation particularly severe in the case of semiconductor lasers [11]. In the past, researchers tried to solve this shortcoming by either implementing some digital phase-frequency devices to extend the capture range [1,3,4,12,13] or adding a Fabry–Perot cavity to pre-reduce the laser jitters [8,14], despite the fact that the digitizing noise mentioned previously could easily

Optics EXPRESS

break the phase locking and an optical cavity would increase the complexity of the optical system. We here introduce a simple approach, using all-analog electronics, to realize sub-millihertz (mHz)-level offset locking with high robustness, i.e., a large capture range. Two different "high-precision frequency transfer" experiments were demonstrated via our offset locking systems: one is to transfer the laser frequency stability from a cesium-stabilized 884-nm diode laser to another 884-nm diode laser whose frequency was seriously jittered previously and the other is to transfer the frequency accuracy of a fiber comb laser to a 778-nm CW diode laser. Our offset locking played an important role in resolving atomic two-photon spectra and we achieved record resolution as will be shown in section 3, though the locking precisions were far beyond those required. When sub-mHz-level offset locking was not required in some other experiments, we proposed an extended design in section 4 and showed the improvement of two-laser coherence by observing the linewidth narrowing in a quantum-interfered system, i.e., electromagnetically induced transparency.

2. Principle

Fabricating a device to serve as a frequency-to-voltage converter is essential for laser offset locking. We show that some simple passive electronics can be used for this. The concept is illustrated in Fig. 1, in which the inset surrounded by a dashed line displays a practical setup of the band pass filter. V_{in} in Fig. 1 stands for the beatnote with beat frequency ω and V_a denotes the signal after passing through the band pass filter, which can be described as

$$\frac{V_a}{V_{in}} = \frac{1}{\sqrt{2}} Z_0 \cdot e^{i(\omega t + \theta_a)} \tag{1}$$

where $Z_0 = \frac{1}{\sqrt{1+\alpha^2}}$ and $\theta_a = \tan^{-1} Z_0$; $\alpha = \frac{R}{\omega L}(1-\omega^2 LC)$; L is the inductance and C is the capacitance.

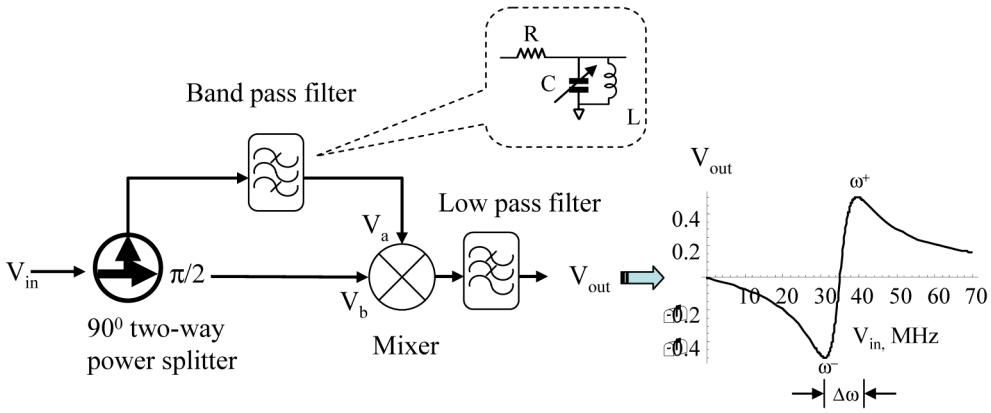

Fig. 1. Basic concept of "self-referenced" frequency-to-voltage converter. V_{in}: beatnote from two lasers. V_{out}: the error signal for feed-back controlling slave laser frequency. Right-bottom: simulation result of V_{out} against V_{in}; Δω: frequency difference between the two turning points ω_+ and ω_-. Dashed inset: band pass filter with R = 910 Ω, C = 20.6 pF, and L = 1 mH. We used a two-way 90° power splitter.

"V_a" is then mixed with "V_b" after a mixer where "V_b" can be maintained at a π/2 phase difference with respect to V_{in} by using a 90° two-way power splitter [15] and "V_b" can be expressed in the form:

Optics EXPRESS

$$\frac{V_b}{V_{in}} = \frac{1}{\sqrt{2}} \cdot e^{j(\omega t + \pi/2)} \tag{2}$$

The DC term of the mixed signal, denoted as V_{out}, can be extracted by applying a low-pass filter and is expressed as:

$$V_{out} = \mathrm{Re}(Z_0 e^{j(\theta_a + \pi/2)}) = \sqrt{\frac{1}{1+\alpha^2}} \cos(\cos^{-1}(\sqrt{\frac{1}{1+\alpha^2}}) + \phi), \tag{3}$$

where the 0.5 $(V_{in})^2$ is normalized to one unit. The right-bottom part of Fig. 1 simulates the trace of V_{out} as a function of the lasers' beat frequency ω. The asymmetric function of ω can serve to stabilize the beatnote. The related turning point ω^+ at the higher frequency side, indicated in Fig. 1, can be derived as:

$$\omega^+ = \frac{\sqrt{2}}{2RC} + \sqrt{\frac{1}{2R^2C^2} + \frac{1}{LC}} \tag{4}$$

and the lower-frequency turning point ω^-can also be derived as:

$$\omega^- = -\frac{\sqrt{2}}{2RC} + \sqrt{\frac{1}{2R^2C^2} + \frac{1}{LC}} \tag{5}$$

The expected frequency instability Δf in the offset locking is proportional to $(\omega^+ - \omega^-)$ and inversely proportional to the signal-to-noise ratio (SNR) of the error signal V_{out}. Therefore, Δf can be estimated as:

$$\Delta f = \frac{\omega^+ - \omega^-}{SNR} = \frac{\sqrt{2}/RC}{SNR} \tag{6}$$

Note that $(\omega^+ - \omega^-)$ is inversely proportional to the Q factor of the band-pass filter, but this does not mean that a larger RC (and thus smaller $(\omega^+ - \omega^-)$) is a better choice for offset locking, since the frequency capture range would be smaller. In the practical situation mentioned in section 3, the frequency capture range was observed to be approximately six times the value of $(\omega^+ - \omega^-)$. Therefore, the trade-off between the capture range and frequency instability in our band-pass filter system (BPS)-based offset locking is inevitable. In our case, we could stabilize the offset frequency to an instability of ~2 kHz at a 1-s integration time by using the BPS alone ($(\omega^+ - \omega^-)$ ~8 MHz) and the capture range was measured as ~50 MHz. Further frequency stabilization was accomplished by a mixer-based system (MBS) that can provide both the accuracy of locking frequency and a tight phase locking to sub-mHz-level beatnote linewidth. The most noticeable feature of our approach is its robustness, that is, the large capture range. The offset lock never broke unless the laser mode hopped. The laser offset locking, as illustrated in Fig. 2 where two 884-nm diode lasers were chosen for the demonstration, was applicable to each laser system mentioned in this paper. Detailed descriptions in Fig. 2 will be mentioned in section 3.

3. Offset locking different laser systems and applications to related high-precision two-photon spectroscopes

Semiconductor lasers are widely used in the AMO field in spite of the fact that they normally exhibited serious frequency–phase jitter [11]. In our laboratory conditions, we were not able to phase lock our two home-built, free-running ECDLs for more than 1 min if only an MBS was employed. In contrast, by adding the BPS mentioned in section 2 to extend the capture range of the MBS, the beatnote between the two diode lasers could be locked for more than 2 hours until the PZT installed in the laser cavity reached its maximum stretching length, owing

Optics EXPRESS

to the surrounding temperature drift. Figure 2 (a) shows the phase–frequency jitter of the free-running

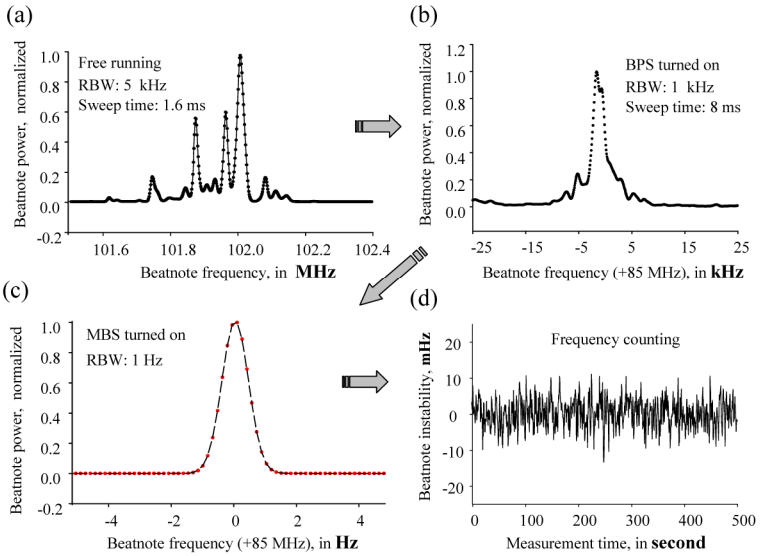

Fig. 2. Demonstration of the step-by-step offset locking. (a): frequency jitter of beatnote; two lasers in freely running; RBW: resolution bandwidth; (b): BPS in Fig. 1 was employed; note that the beatnote was captured from 102 MHz in (a) all the way down to 85 MHz and was then frequency-stabilized; (c) the beatnote in (b) was further stabilized via MBS; resolution was limited by the RBW of our RF spectrum analyzer [16]; (d) Beatnote frequency instability; the precision was limited by the time base instability of counter. In normal situation, the error signals from BPS and MBS were summed up together for feeding back.

beatnote, recorded from a spectrum analyzer [16] with 5-kHz resolution bandwidth and 1.6-ms sweep time. When the beat frequency of the two lasers approached 85 MHz and fell in the 25-MHz capture range, we activated the BPS-based feedback loop. The beatnote was then rapidly pulled toward 85 MHz and was frequency-stabilized with a 2-kHz frequency instability, as shown in Fig. 2 (b). Since the BPS used in Fig. 2 was the same as that illustrated in Fig. 1, an additional synthesizer and mixer were needed to lower the beat frequency to the band-pass frequency (35 MHz). Further optical phase locking was performed by activating the MBS. The beatnote linewidth is shown in Fig. 2(c), while the resolution bandwidth (RBW) of our RF spectrum analyzer was limited to 1 Hz [16]. The beat frequency (85 MHz) was directly recorded by a frequency counter whose time base was independently used, as shown in Fig. 2(d). Figure 2 is for showing the individual locking ability of the BPS and MBS. Practically, the error signals from BPS and MBS were summed up together for feeding back to laser.

The 16-mHz frequency fluctuation (standard deviation) in Fig. 2(d) was considered as coming from the uncorrelated phase noise of the time bases between synthesizers and frequency counter. To verify this, it is necessary to carefully analyze the consequence of our offset locking by the other experimental arrangement shown in Fig. 3, where the time bases of all synthesizers were phase-locked together. The master laser and slave laser used in Fig. 2 and Fig. 3 were two home-built 884-nm ECDL diode lasers whose linewidths were about 200 kHz and long-term frequency drift was about 100 MHz/min (back and forth) in freely running. The beatnote linewidth was recorded by heterodyning the beat frequency down to 10 Hz with the use of Syn #1, as shown in Fig. 3. Syn #2 was used to lower the 85-MHz beat frequency to 35 MHz, which was the central frequency of the BPS. When the frequency of Syn #2 was linearly changed with

Optics EXPRESS

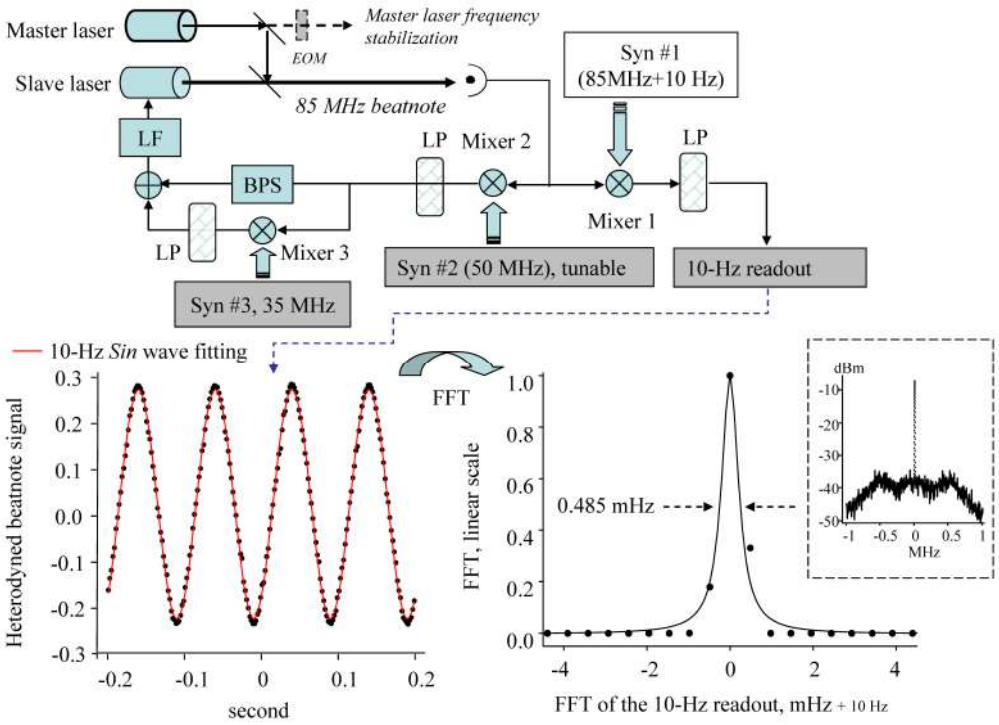

Fig. 3. Experimental setup for showing the ultimate beatnote linewidth in our offset locking. BPS: band-pass system; LF: loop filter; LP: low-pass filter; Syn: synthesizer; bottom-left: part of the time-domain readout from mixer #1 where the solid-red fitting curve is a pure 10-Hz sinusoidal wave (2-ms averaging time for each data point). The total data acquisition time was actually 2.5 h; bottom-right: FFT spectrum transformed from the acquisitioned date stored in the hard disk. Inset is the log-scale power spectrum that extends the spectral range from 8 mHz to 1 MHz, from which one can deduce the phase noise [17,18].

time, the beat frequency was linearly tuned accordingly, as a result of which the tuning range in our offset locking could be up to several gigahertz, limited by the working range of Syn #2 and mixer #2 as well as the detection bandwidth of the photodiode. The phase of beatnote was eventually locked against Syn #3 via mixer #3. The 10-MHz time bases of all synthesizers were locked together and referenced to Syn #3. The bottom-left part of Fig. 3, in which the time-domain data was fitted by a pure 10-Hz sinusoidal wave (red line), displays part of the beatnote that was extracted from 2.5-hour data storage. The bottom-right part of Fig. 3 shows the fast Fourier Transform (FFT) spectrum transferred from the entire 2.5-hour time-domain data. The fitted Lorentzian curve (black line) in the bottom-right part of Fig. 3 has a linewidth of ~0.5-mHz. Similar results were also observed in the other laser systems mentioned in this paper.

Although the optical frequency of the slave laser had already precisely followed that of master laser, phase noise [17,19] existed as shown in the inset of Fig. 3. The limitation for not being able to further improve the coherence between the two lasers was not due to the sensitivity of our approach, but due to the limited frequency bandwidth (400 kHz) of our feedback loop. The root mean square phase noise $<\Delta\phi^2>$ of the beatnote, deduced from the inset of Fig. 3, is ~60 milliradians [4,17,19].

When the master laser in Fig. 3 was a 884-nm ECDL laser, one EOM (electro-optical modulator) with a 152-MHz modulation frequency was used and its −1 order sideband was frequency-dithered for stabilizing the sideband frequency to cesium atom $6S_{1/2}$, F = 4 → $6D_{3/2}$, F' = 4 two-photon transition [20]. The EOM was implemented to avoid a zero offset frequency as the laser frequency was scanned over the entire hyperfine spectra. As the master

Optics EXPRESS

laser was pre-stabilized by this sideband-dithered EOM [20], the beatnote between master laser and slave laser was actually not dithered since the un-modulated laser beam before passing through the EOM was used. In the other case that the master laser was a frequency-doubled 1.5-μm fiber comb laser, no EOM was needed and the slave 778-nm diode laser frequency was directly offset locked by one mode of the comb laser.

Figure 4(a) shows the spectrum resolved by the aforementioned 884-nm slave laser, in which the

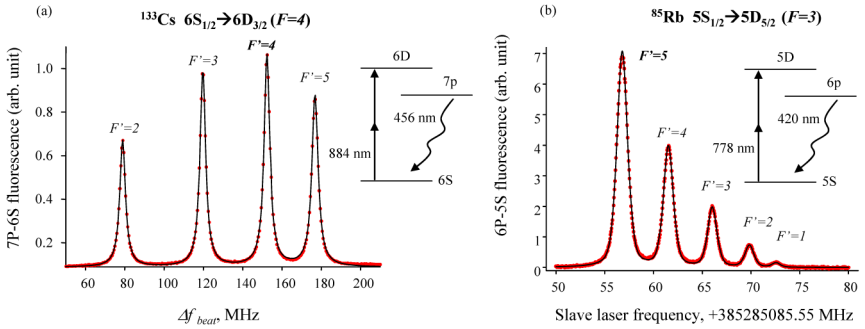

Fig. 4. The applications of our offset locking on two-photon spectra: different atoms with the relevant energy levels, respectively. Black solid lines are Lorentian fitting; (a) spectrum resolved by 884-nm intracavity slave laser; (500 kHz per frequency step). Δf_{beat}: beat frequency between the master and the slave laser illustrated in Fig. 3; (b) spectrum resolved by 778-nm intracavity slave laser which was offset locked to the second harmonic of a 1.5-μm fiber comb laser (50 kHz per frequency step); no EOM is needed in this case. Note that the cold finger temperature was room temperature (23°C), see text.

transverse axis shows the beat frequency (Δf_{beat}) between the master laser and slave laser. In this case, the BPS frequency was set to be 35 MHz and a high-speed operational amplifier was used right after the BPS to further improve the input impedance. The slave laser we employed here was an intra-cavity cesium spectrometer and the laser structure was the same as that mentioned in [18]. That is, a Brewster-angle-cut cesium cell was implemented inside the slave-laser cavity. The "offset lock" played an important role in step-by-step resolving the unperturbed hyperfine lineshapes of the cesium $6S_{1/2}$-$6D_{3/2}$ transitions, by changing the frequency of Syn #2 in Fig. 3. The hyperfine intervals can be obtained from Fig. 4(a) and are listed in Table 1, where the results of previous works are compared. From Table 1, one can find that our "offset-lock approach" yielded a precision one order of magnitude higher than that in previous works. From the hyperfine intervals in Table 1 we derived new values of hyperfine constants A and B. The definitions of A and B are the same as those used in [21,22], that is, A is the nuclear magnetic dipole coupling constant in the hyperfine Hamiltonian as

$$H_{dipole} = AI \bullet J \tag{7}$$

and B stands for the quadrupole-moment coupling constant in the hyperfine Hamiltonian as

$$H_{quadrupole} = B\frac{3(I \bullet J)^2 + \frac{3}{2}(I \bullet J) - I(I+1)J(J+1)}{2I(2I-1)J(2J-1)}. \tag{8}$$

Table 1. Cesium 6D3/2 hyperfine intervals derived from Fig. 4(a), Lorentzian fitting.

Intervals	This work	A. Kortyna, et. al. [21]	T. Ohtsuka et. al. [22]
F' = 2, 3 (MHz)	81.66 ± 0.02	81.8 ± 0.1	81.15 ± 0.42
F' = 3, 4 (MHz)	65.28 ± 0.01	65.1 ± 0.2	64.18 ± 0.25

Optics EXPRESS

F' = 4, 5 (MHz)	48.88 ± 0.02	49.0 ± 0.1	48.76 ± 0.32
Hyperfine constant A	16. 3331 ± 0.008	16.34 ± 0.03	16.17 ± 0.17
Hyperfine constant B	–0.36 ± 0.01	–0.1 ± 0.2	0.11 ± 0.13

The uncertainty in determining the hyperfine constants mainly came from statistical errors; the other systematic errors were also studied and are listed in Table 2. Note that our study is only on a single cell; hence, Table 2 does not include the error from different cells, though [20] had proved that, for cesium 6S–8S hyperfine transitions, different cells only influenced the transition frequencies, not the determination of hyperfine constants.

Table 2. Error budget for determining the hyperfine constants A and B*

	Statistic	Master laser	Cesium cell system (intra-cavity scheme)		
		Freq. instability	Pressure shift	Magnetic field	Light shift
influence in *A*	6 kHz	38 Hz	26 Hz	< 8 Hz	237 Hz
influence in *B*	10 kHz	–56 Hz	603 Hz	< 12 Hz	349 Hz

* the error budget does not include the errors from different cells, which are considered as negligible in the 6S-8S transition [20], see text. Beam overlapping is supposed to be perfect in laser cavity.

Similar offset locking can also be realized in other laser systems, such as a 778-nm intracavity diode laser [18] offset locked by a frequency-doubled fiber comb laser. That is, the diode laser frequency can be referenced to that of a comb laser whose repetition rate is directly referenced to a cesium atomic beam clock [23]. By changing the offset frequency between the comb laser mode and diode laser, the optical frequency of the offset-locked 778-nm diode laser could thus be changed and a set of unperturbed hyperfine transitions in atomic ^{85}Rb, as shown in Fig. 4 (b), could thereby be resolved. The integrating time of each data point shown in Fig. 4(b) was 0.5 s and the laser frequency step was 50 kHz/step, which led to a record SNR at room temperature (23 °C cold finger temperature). Note that the SNR shown in Fig. 4(b) was from three orders of magnitude fewer atoms [24] than that of the spectra resolved from the standard transition (90 °C cold finger temperature) [25–28]. The ultra-high SNR proves the significance of our approach in resolving the nonlinear spectra.

4. Extended design and the influence on EIT experiment

An extended design based on notch (band-reject) filter is shown in Fig. 5(a) for improving the inevitable situation described at the end of section 2, where the problem of trading off between capture range and frequency stability was addressed. Many AMO experiments do not need a further MBS to solve this dilemma since sub-mHz and absolute frequency are not critical in their experiments. Instead, they only require more robust and sub-kHz-level offset locking. The extended design in this section satisfies this second requirement with no need of any frequency synthesizer. The idea is shown in Fig. 5 where the band pass filter in Fig. 1 was replaced by a notch filter. Since the reflected RF signal did not actually heat the notch filter, the resulting SNR was unaffected by the thermal noise caused by the filter.

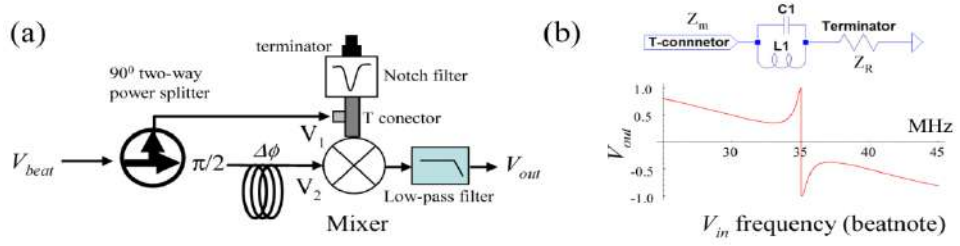

Fig. 5. (a) Extended design for enlarging capture range and improving frequency stability compared to the design in Fig. 1(b) Simulated curve using the lowest-order notch filter shown in upper part; C_1: 2.06 nF; L_1: 10 nH; Z_m and Z_R: 50 Ω.

The calculation is just similar to what has been discussed in section 2 except that an additional delay line having 2π phase delay at 35 MHz [29] was included. The simulated V_{out} is displayed in Fig. 5(b) where 10-nH inductance and 2.06-nF capacitance were used. The slowly varying curve from 25 MHz to 45 MHz is due to the wave number-dependent phase delay line [29] and the narrow dispersed curve from 34 MHz to 36 MHz is due to the bandwidth of the notch filter. In a practical situation, a commercial band-reject filter was employed [30] to lock the beatnote. When the offset locking was activated, even more robust frequency locking than the aforementioned BPS was observed, with sub-kHz-level offset frequency instability and without the need of the MBS system mentioned in section 2. Figure 6 shows the proof of the improvement of light phase coherence, inspected by an atomic quantum interference system referred to as EIT. The optical setup is similar to that of [3], except that we did not shield our room-temperature cesium cell from the influence of the earth's magnetic field.

The coupling laser used in Fig. 6 was frequency-stabilized to the $F = 4 \rightarrow F' = 3$ hyperfine

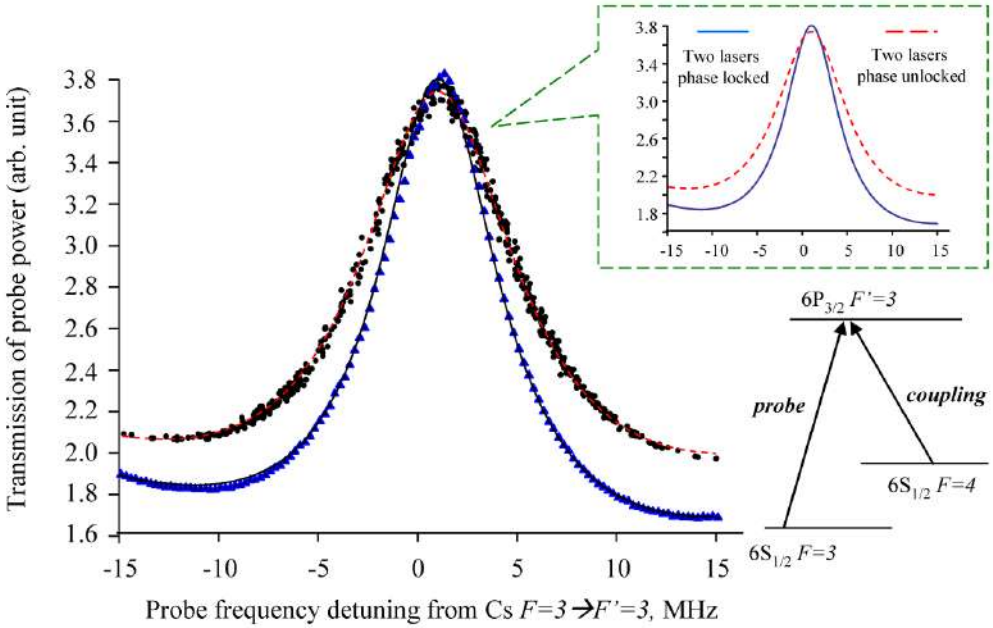

Fig. 6. EIT signal resolved via the offset-lock scheme shown in Fig. 5, with the fitted curves in inset (right-upper). Right bottom: the relevant level diagram; Black scattered dots were recorded as probe laser was freely wondering around the $3 \rightarrow 3$ transition; Blue tri-angle data: probe laser was offset-locked to coupling laser where the offset frequency was tuned to 250 kHz/step, see text; probe power: 0.2 mW; coupling power: 6 mW.

transition by modulation transfer spectroscopy [31]. A portion of the coupling light (un-modulated) was conducted to offset lock the probe laser via the locking method illustrated in Fig. 5. Eventually, a combined laser beam with 6-mW coupling power and 0.2-mW probe power was sent into a cesium cell and the transmitting probe light, having polarization perpendicular to that of the coupling light, was reflected by a polarization beam splitter such that the transparency at resonant frequency could be detected. First, in preparing two incoherent light sources, we let the probe laser be in freely running and simultaneously recorded the beat frequency between the probe laser and coupling laser. The transparent-window part was recorded in Fig. 6, scattered black dots with a red-dashed Lorentzian fitting where the fitting included the Gaussian background of $F = 3 \rightarrow F' = 3$ and nearby transitions. The transmitting intensity of probe light was averaged at 0.1 s sampling time, which was the

Optics EXPRESS

same as the gate time of the frequency counter we used. The inset shows a clearer trace of the fitted red-dashed line that has (9.7 ± 0.1) MHz Lorentzian-part linewidth (FWHM) and 1.04 ± 0.01 MHz frequency shift. Since the coupling laser was frequency locked, the transverse axis in Fig. 6 shows the detuning of the probe beam from the $F = 3 \rightarrow F' = 3$ hyperfine transition. For contrast, we let two lasers be phase locked via the approach mentioned in Fig. 5 and the offset frequency was tuned step-by-step with 250 kHz /step. The triangle data in Fig. 6 displays a narrower transparent window due to the improvement of two-light coherence, showing high agreement with the theoretical curve (blue solid line), which has 7.35 ± 0.05 MHz (FWHM) Lorentzian-part linewidth and 1.049 ± 0.008 MHz frequency shift. The two frequency shifts between red dashed and blue solid lines were the same since the two experiments were performed under the same conditions except for the coherence between two lasers. In our experimental situations, the frequency shifts of two EITs mainly resulted from the same light intensity shift [32]; the transparent width could not be further reduced since it mainly resulted from AC-stark broadening and power broadening [33,34].

5. Conclusion

With all-analog electronics, we successfully showed that sub-Hz-level optical offset locking in normal laboratory conditions (i.e., no atomic clock) was feasible, as illustrated in Fig. 2. The experimental result in Fig. 3 proved that optical phase-frequency transfer at the sub-mHz level is achievable with our simple devices, once the time bases of the related synthesizers referred to the primary time standards. Various two-photon spectroscopes were realized, in which the excellent offset locking played an important role. In other words, we demonstrated that, when the master laser was frequency-stabilized and the slave laser tightly followed the phase-frequency of the master laser via robust offset locking, ultra-high resolution in weak transitions were achievable since the slave laser frequency was able to be step-by-step tuned with accurate frequency position at each step and with long-enough sampling time for each data point in the spectrum. Therefore, robust offset locking was vital in those applications to nonlinear spectroscopy since the slave laser could be high power and un-modulated while maintaining the same frequency stability as that of the master laser. The spectral demonstrations in this paper not only show the good performance of our offset locking but also helped to develop a general approach for resolving high-resolution unperturbed nonlinear spectra, which is particularly advantageous for those researching systems having weak transition amplitudes and narrow linewidths. Note that, a similar idea was implemented by R. L. Barger and J. L. Hall in 1969 in which a saturation dip spectrum of with linewidth as narrow as 150-kHz was nicely carried out [35], showing even wider impact of offset locking on laser spectroscopy

Improvements are being made to the repetition-rate stability of our comb laser. That is, we plan to phase lock the Ti:sapphire comb laser repetition rate directly against a cesium-stabilized 822-nm diode laser [36] that is similar to the “iodine clock” approach [37]. The short-term frequency stability of the 822-nm diode laser will refer to a high-stability optical cavity and the long-term frequency stability will refer to a cesium atom 6S-8S two-photon transition whose absolute frequency has been carefully studied [20]. Again, the key aspect would be the offset locking between a comb laser and CW laser.

Funding

Ministry of Science and Technology (MOST) (101-2112-M-008-015-.)

Optics EXPRESS

Acknowledgments

We are grateful to Chunghwa Telecommun. Labs, which provided us the cesium atomic clock; We appreciate Dr. Ming-Sheng Chang and Dr. Ying-Chen Chen in IAMS (Acdemia Sinica, Taiwan) for kindly lending us the Oscilloscope and spectrum analyzer mentioned in this paper; the AMO focus group of Ministry of Science and Technology (MOST) and the CQSE of National Taiwan University, which offered nice platforms for useful communications research.